Accepted Manuscript

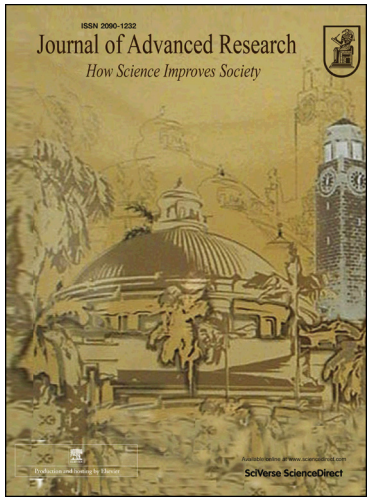

Original Article

The Study on Force, Surface integrity, Tool life and Chip on Laser Assisted Machining of Inconel 718 using Nd:YAG laser source

K. Venkatesan

PII: S2090-1232(17)30055-3
DOI: http://dx.doi.org/10.1016/j.jare.2017.05.004
Reference: JARE 532

To appear in: *Journal of Advanced Research*

Received Date: 16 February 2017
Revised Date: 10 May 2017
Accepted Date: 11 May 2017

Please cite this article as: Venkatesan, K., The Study on Force, Surface integrity, Tool life and Chip on Laser Assisted Machining of Inconel 718 using Nd:YAG laser source, *Journal of Advanced Research* (2017), doi: http://dx.doi.org/10.1016/j.jare.2017.05.004

The Study on Force, Surface integrity, Tool life and Chip on Laser Assisted Machining of Inconel 718 using Nd:YAG laser source

K. Venkatesan*

School of Mechanical Engineering,

VIT University, Vellore 632014, India

Email address: venkatesan.kannan@vit.ac.in

Abstract

Inconel 718, a high-temperature alloy, is a promising material for high-performance aerospace gas turbine engines components. However, the machining of the alloy is difficult owing to immense shear strength, rapid work hardening rate during turning and less thermal conductivity. Hence, like ceramics, and composites, the machining of this alloy is considered as difficult-to-turn materials. Laser assisted turning method has become a promising solution in recent years to lessen cutting stress when materials that are considered difficult-to-turn, such as Inconel 718 is employed. This paper investigated the influence of input variables of laser assisted machining on the machinability aspect of the Inconel 718. The comparison of machining characteristics has been done to analyze the process benefits with the variation of laser machining variables. The laser assisted machining variables are cutting speeds of 60–150 m/min, feed rates of 0.05-0.125 mm/rev with a laser power between 1200W and 1300W. The various output characteristics such as force, roughness, tool life and geometrical characteristic of chip are investigated and compared with conventional machining without application of laser power. From experimental results, at a laser power of 1200W, laser assisted turning outperforms conventional machining by 2.10 times lessening in cutting force, 46% reduction in surface roughness as well as 66% improvement in tool life when compared that of conventional machining. Compared to conventional machining, with the application of laser, the cutting speed of carbide tool has increased to a cutting condition of 150 m/min, 0.125 mm/rev. Microstructural analysis shows that no damage of the subsurface of the workpiece.

Keywords: laser assisted machining; PVD-AlTiN; cutting forces; surface integrity; tool life; chip formation

Introduction

Components owing to their high strength like titanium alloys, nickel alloys, composites, and ceramics are found as critical parts of their equipment in automotive, space, and nuclear industries on the basis of appreciable thermo-mechanical characteristics [1]. But, the transformation of such high strength components into industrial parts using conventional machining is very difficult and uneconomical. High heat generation in the cutting area, as well as problems in temperature dissipation due to low heat transfer coefficient of such materials, are main causes that make machining through conventional method a difficult task. Increased hardness, as well as strength at elevated temperature, makes this material difficult to machine that result in considerable tool wear leading to shorter tool life along with deprived surface integrity [2]. A new technique called laser assisted turning (LAT) is introduced and implemented in the field of machining of these materials [3]. Compared the other heating energy sources, induction coil, gas flame, furnace heating, plasma and electricity, the laser is preferred as a heating tool for turning due to precise control of heat concentration and easy-to-control of scanning parameters. Further, it will minimize thermal effects on the surface of workpieces [2]. In this process, the laser is focused on the workpiece for a small projected area produced controlled laser energy (temperature) anterior of the cutting insert. Temperature obtained is adequate for lessening material yield strength/hardness in the surface layer of the material. The heated volume of material in the radial direction can be removed with conventional tool material thereby improving the machinability benefits.

In past decades, there have been several research works on conventional machining of Inconel 718 alloy to improve machinability. Many researchers used different cutting tool materials for their investigation on machining of Inconel 718 alloy. Among them, carbide

inserts (both coated and uncoated), cubic boron nitride and ceramic are commonly used. Cubic boron nitride (CBN) tools along with their coatings are commonly employed owing to high wear resistance, greater hot hardness along with strength, appreciable heat transfer coefficient as well as better mechanical features when compared to coated carbide tools [4, 5]. But, the higher cutting force is reported for CBN than those the carbide tools [6]. In addition to this, it is reported that the CBN tools are subjected to excessive chipping during machining of Inconel 718 [7]. The polycrystalline cubic boron nitride (PCBN) tools are found to show the higher temperature at rake face during machining of Inconel 718 compared to ceramic tool [8]. In industry, both uncoated as well as coated cemented carbides have been widely used. Titanium-based hard coatings like TiN, TiC, TiCN, TiAlN, and Al_2O_3 are used in the form of coating materials for carbides [9]. This special coating possesses greater oxidation resistance; enhanced chemical stability at elevated temperature; increased hot hardness as well as low heat transfer coefficient during machining of Inconel 718 [10]. Application of coating materials to the cutting tool has been carried out by employing two disparate processes: chemical vapour deposition (CVD) and physical vapour deposition (PVD). PVD being less costly that of CVD, in fact, provides better coating properties [9]. Further, these coatings lessen the built-up-edge formation, tool wear ploughing, plastic deformation and other surface defects like grooves, white layer formation and surface tensile residual stress [10]. Multilayer PVD coated carbide tools provides an enhanced performance in the life of tool when compared to that of single layer PVD coated carbide tools during turning of Inconel 718 [11]. The tool life of uncoated carbide insert is noticed as half that of multi-layer coated carbide tools during turning of Inconel 718, and surface roughness of the coated tool is lower [12]. PVD-coated carbide tools are recommended when compared to that of ceramic tools having negative rake angle because of their lower cost. However, it was thus concluded that a limited speed of 30-50 m/min should be the optimal value in dry machining

of Inconel 718 alloy with a PVD (AlTiN) coated carbide tool for giving the acceptable surface quality [13, 14]. AlTiN coated tool have superior properties than other coated carbide tool as it possesses higher hardness at elevated temperature (T ≥ 750ºC). From the review of the literature, the PVD coated AlTiN carbide cutting tool is used for the present investigation.

However, the exploratory data on LAT of Inconel 718 is turned on both ceramics and coated carbide insert. Comparing the conventional machining (CM), during LAT of Inconel 718, a reduction in cutting force along with improvement in the life of tool by about 25% and 200-300% respectively is obtained by increasing the cutting temperature of about 540ºC using ceramic insert [15]. At cutting speed along with feed rate up to 300 m/min and 0.3 mm/rev respectively with fixed laser power of 3000W, when using the SiAlON ceramic tool with Nd:YAG laser source for the same material, results in cutting temperature rise (650°C), lessening in surface roughness (25%) and enhancement of material removal rate (800%). The flank wear and adhesion are the dominant wear modes while chipping and crater wear on the rake face have not found [16]. The mechanism involved for lower the strength and position of a laser source for cutting force is examined further on Inconel 718 using Nd: YAG laser source. The decrease in cutting force (≈18%) is reported by employing laser power of 2000 W while positioning the laser spot to the cutting tool of about 45 mm [17]. In the same author, due to excessive heating, the life of tool of CVD carbide has been found to be lower in LAT of Inconel 718 that of CM. A similar result on tool life of CVD carbide insert is confirmed using Nd: YAG laser source [18]. In the same study, the life of ceramic inserts during LAT of Inconel 718 is increased by 25% that of CM. Therefore, an optimal laser power and beam orientation are required for coated carbide insert to get the longest life of tool in order to prevent the tool insert from overheated due to the reflectivity of the laser beam radiation on the surface of the workpiece against the cutting tool. In this direction, further research on improvement in machinability is examined by authors [19-23].

The simultaneous effect of laser scanning parameters like speed, feed, laser power along laser beam angle on preheating temperature (Ts) and heat affected depth (HAD) is examined on Inconel 718 alloy using Nd: YAG laser. Reported that increment in HAD is noticed due to increment in the laser power and decreased due to the increment of the laser beam angle, speed, along with the feed. The desired surface temperature of 750°C- 860°C for LAT experiments of Inconel 718 alloy is achieved at an approach angle of 60° and laser power 1250 W-1500 W [19]. Laser moving heat source is studied at an angle of 'θ' from the surface for Inconel 718 using Nd: YAG laser source. The cutting tool employed in the investigation is CVD ($TiCN/Al_2O_3/TiN$). Of the variance test, laser beam angle along with laser power are the predominant variables that influence the machining forces as well as cutting temperature. The optimal points, which increasing the cutting temperature up to 860ºC, can enhance tool life by 43% as compared to that of CM [20]. At an approach angle of 60° laser spot, using LAT of Inconel 718 alloy with CVD ($TiCN+Al_2O_3+TiN$), there was no significant variation in hardness value prior to and after LAT [21]. Further experimented on Inconel 718 using Nd;YAG laser source with PVD (TiAlN) coated insert at an approach angle of 60° and results reveals about the extended tool life up to 133% that of CM at the determined optimal parameters [22]. The results of the substrate and subsurface analysis showed that the surface finish on Inconel 718 is not been affected by heat during CM and LAT [23]. At the beam orientation of 35°, the measured cutting forces and minimum uncut chip thickness are increased along with lessened tangential force increments with the increment in cutting speed during LAT of WC/NiCr clad layer [24]. At tool's angular distance from the laser beam of 45° and cutting depth of 0.05 mm, the application of laser power results in the process benefits of 32% in case of roughness and 27 % in case of wear rate during machining of A359/20SiCP metal matrix composite [25]. Cryo-machining, on the other hand, drops down the conventional cutting temperature to a greater extent and lower the

surface roughness by 30% and 40% than that of flood and dry machining in addition to it prompts surface work-hardening of workpiece [26]. But interestingly, PVD (TiN/TiAlN) coated tool reduced cutting force 40% and 16% under dry environment when compared with the flood as well as other MQL environment [27]. Recent reports reveal that the machining cost in association with the use of cutting fluid contributes to a maximum of about 20% in comparison with the tool cost whose percentage is estimated approximately around 4% [28]. Therefore, in the current study, dry machining is chosen as primary objective on Inconel 718 as it striving by the comprehensive endeavor to minimize or eliminating cutting fluid usage.

From the studies of LAT on Inconel 718, predictive models, simultaneous effects, and multi-objective optimization of speed, feed, laser power, along with laser approach angle was investigated [19-23]. The maximum benefit in terms of machinability can be achieved at 60° laser approach angle and by increasing the laser power up to 1300 W since that heat-affected area in the final machined workpiece will be present at a cutting depth of 0.5 mm. But, no reported literature on LAT of Inconel 718 alloy using AlTiN PVD coated tool to study the process benefits beyond the cutting speed of 60 m/min based on investigated experimental results at 60° laser beam angle [19-23]. Thus further study on LAT is required to establish a conclusive result for better process benefits of such difficult to machine alloys. In this context, LAT experiments are conducted to examine the possibility of broadening the process benefits on cutting forces, surface integrity (surface roughness and subsurface damage), tool life, and chip morphology beyond 60 m/min. The result is compared with conventional machining to reveal the machinability improvement. Furthermore, tool failure and subsurface microstructural integrity of the workpiece has been analyzed.

Experimental

Workpiece and cutting tool

Workpiece material employed in present research is Inconel 718 superalloy with an average measured material hardness of 48 HRC. The cylindrical workpiece of 25 mm diameter and 300 mm length is used for each machining trials. Inconel 718 alloy has been used for jet engine and high-speed airframe parts such as discs, casings, blades, impellers, rings shafts, and high-temperature bolts and fasteners. Machinability of these components includes many machining methods for conversion of final engineering products. For example, casings and discs consist turning of about 60% and 45% that of milling (35%) and drilling (5%) [29]. Hence, this paper is focused on laser assisted turning of Inconel 718. The cutting tool used is PVD coated (AlTiN) carbide inserts. The specification of cutting insert and tool holder is CNMG 120408-MS-KU25 and PCLNR 2020 K12 respectively. AlTiN has a significantly higher hot hardness of above 750°C. At 1000°C, AlTiN is considerably harder compared to TiCN and TiN [11]. The higher hot hardness of AlTiN coatings is due to the solid solution effect of either carbon or aluminum in the TiN lattice. It also exhibits good chemical stability at elevated temperature and has high resistance to abrasive wear. 'PCLNL2020 M12' type tool holder is employed having tool geometry: tool major cutting edge angle=80°, back rake angle=−6°, clearance angle=5°, approach angle=95° and nose radius=0.8 mm.

Experimental setup

The laser assisted machining system consists of Nd: YAG continuous wave laser source having highest power of 2 kW and high-speed lathe having the highest spindle speed of 3600 rpm. It is class IV laser systems that produce a single wavelength (1064 ± 10 nm); a

laser beam at power levels up to 2 kW without modulated. Mounting of laser head is carried out upon a specially designed fixture that is further synchronized with tool holder in feed direction for axial movement. The positioned laser head on the fixture delivers the laser beam in such a way that the laser beam center always strikes the centerline of the cylindrical workpiece during scanning. The laser head is set at the angle of 60° circumferentially on workpiece surface ahead of the cutting tool of 2 mm. The beam is targeted by fiber optic cable using a lens having a spot size of 2 mm. The surface temperature of the workpiece is recorded continuously using a dual wavelength infrared pyrometer. The cutting force Kistler dynamometer is attached to the tool post. A circular spot contour size of 2 mm diameter is kept because of less heat transfer coefficient of Inconel 718 alloy as well as to prevent high heating that influences edge of the cutting tool [19]. The distance between the laser optic head to cutting tool distance is kept at 200 mm and the laser spot beam pattern of circular is focused onto the workpiece just ahead of the cutting tool with positioned approximately 2 mm. As a result, workpiece material gets heated directly in front of the cutting tool. Fig. 1(a) displays schematic view of laser assisted turning system.

Machining trials

In the present investigation, cutting speed (S), feed rate (f) and laser power (P) are considered as the laser machining parameters that influence a variety of machinability features like machining forces (Fz, i.e. perpendicular direction of the cutting tool axis) in operation, workpiece surface roughness (Ra) as well as flank wear (Vba) in cutting tool. According to presented study, the levels of parameters are as follows: two levels of laser power (1200 and 1300 W), four levels of cutting speeds (60, 90, 120, and 150 m/min) and two levels of feed rate (0.05 and 0.125 mm/rev) with a cutting depth of 0.5 mm. To avoid phase transformation even at the under of tool life criteria of 0.3 mm according to ISO 3685

in the final machined workpiece, a laser power maximum of 1300 W is not exceeded during LAT based on the investigated experimental results [19-23]. It is determined experimentally that this laser power cannot upsurge cutting temperature at given cutting depth beyond the critical cut-off cutting temperature selected for phase transformation, that ranges from 760°C – 860°C for workpiece zone preheating wider than 0.5 mm. It also reported that there is no change in the hardness value (48 HRC) of the machined surface due to laser heating [21]. The average surface temperature of the sample just before engaging the cutting insert is measured using pyrometer as shown in Fig. 1(a). Results and/or plots of average surface temperature for machining trials are discussed in tool wear analysis section. To extract the surface temperature values, the emissivity value of an Inconel is assumed as 0.46 in the present study [17] and the time rate for temperature rising is set approximately 10-15 seconds. Further, surface temperature decreased to 760 to 538°C when the feed rate is increased beyond 0.125 mm/rev [19]. So the feed rate is selected between the ranges of 0.05-0.125 mm/rev in the present study.

Methodology

The machining experiments are stopped for both the conditions (CM and LAT) when the tool flank wear value reaches the criteria of 0.3 mm according to ISO 3685. Cutting forces, surface roughness, tool flank wear along with surface integrity (microstructure) relying on machining length, data is developed approximately at each length of cut of 50 mm. Using an optical microscope, tool flank wear is measured for every 50 mm length of cut during the tests, then the tool is returned to the tool holder and the test restarted. Force is measured continuously by employing Kistler dynamometer 9257B type having digital indicator connection with computer data acquisition system. Surface roughness value is

measured for every length of cut by employing Mahr surf test (Model GD120). The process flow chart of experimental steps is shown in Fig. 1(b).

The subsurface microstructural analysis is done by employing an optical microscope. The etchant is a Keller's solution (5 ml hydrochloric acid, 3 ml acetic acid, 3 ml of nitric acid and 2-3 drops of glycerol). For subsurface microstructure analysis, small cubical sections (10 mm x 5 mm x 8 mm) of the laser treated workpiece are cut from cylinder bar by employing wire electro-discharge machining. Cut samples are hot mounted in Bakelite and prepared metallographically in order to achieve a mirror-like surface. The subsurface microstructural analysis is conducted with a maximum of 200 × magnification. To know the geometrical parameters of a chip formed during LAT, the chips are collected for both new (during the first cut when the insert of the cutting edge is new) and worn-out; the chips are cut with a small length of 5 mm. It is positioned in such a way that the longitudinal cross-section of the chips is facing upwards (the surface which is to be ground and polished). The polishing of the chip samples is performed using a silicon carbide paper of 220 grit size followed by 9 μm diamond solution for 4 minutes with a force of 200 N and 180 rpm under disc polishing machine. The samples are analyzed under an optical microscope. Then geometrical feature of the chip is measured at three separate locations using the microscope.

Results and discussion

Force analysis

The cutting force is measured for every 50 mm machining length until tool failure criteria. The measured results for both new and worn tool are tabulated in Tables 1 and 2, respectively, under the category of laser power 1200 W, 1300 W vs 0 W, respectively. Comparing the LAT with conventional machining, the magnitude of machining force is found to be lower (Table 1). The temperature rise when the laser power is used resulted in a

reduction in material hardness and/or shear strength which decrease the thermo-mechanical force on the cutting tool edge. Furthermore, the reduction in machining force is observed for both new and fresh tool than the conventional force using neither low nor high power. This may be attributed to the fact that the heat-affected area at a cutting depth of 0.5 mm is effectively removed from the machined workpiece during turning of this alloy when beam placement is done against cutting tool at 60°. In other words, the preheating temperature along with heat affected depth for material using a laser source is effectively controlled under the various combinations of laser machining parameters. However, cutting force decreased with increased in cutting speed and increased by an increment of feed rate for both CM and LAT. In conventional machining, increasing cutting speed, the chip thickness decrease that reduces the cutting force which consequently results in a decrease in cutting pressure on the cutting tool. Increasing feed rate results in an increment of cutting force because of increase in friction as well as the temperature at the chip/cutting tool interface.

In LAT, increasing speed resulted in favouring the contact time between workpiece/ laser and/or softening effect on the volume of removed material increased appropriately probably may be because of the lesser time needed to dissipate heat (low thermal conductivity) thus proportionally lessening the forces as the speed increases. At speed beyond 25 m/min, the laser softening surpasses the rate of strain hardening thus lessens the force with further increment in speed [30]. The employed cutting speeds, in the presented cutting trial, are more than 60 m/min. Thus, the thermal softening influences reduction in force. Generally, increasing the cutting speed lessening the interaction time and consequently, the cutting temperature reached will be lower. But in this case, it favors the material as it reaches the cutting tool, become softer even at the higher cutting speed of 150 m/min and thus resulting in a high reduction in cutting force. But for values exceeding 150 m/min, the interaction time is shorter so that the cutting temperature required attaining descent in the material hardness

and/or yield strength cannot be reached. This result is in agreement with other research work [23]. When increasing the feed rate interaction time of laser beam with material becomes short and thus the cutting temperature decreases. So the thermal softening is minimized, which can be the cause for a lesser cutting force reduction using LAT for the increment in feed rate.

Based on analysis done above, the highest reduction in cutting force (2.10 times) during LAT occurs at the lower feed rate along with higher cutting speed since it has an effective preheating temperature in the primary cutting zone. In the same way, the magnitude of reduction in cutting forces (1.82 times than CM) is observed at the higher feed rate at low cutting speed. This may be the reason due to the increased interaction between the volume of chip and material softening provoked by the laser source. By increasing feed rate along with cutting speed, the reduction in cutting force (0.84 times) is small may be due to the chip volume is small. The similar trend is observed for the worn tool, the laser beam only lessens the value of cutting forces over CM. Additionally, it has to be registered that cutting forces for the worn-out tool at the end of tool life are recorded and tabulated in Tables 1 and 2, respectively. Though it is difficult due to different wear mechanisms, some characteristics are used to interpret the cutting forces variation at the end of tool life. In each operating parameters, cutting forces are found higher for worn-out compared over fresh inserts due to the accumulated tool wear. The cutting force variations are smaller when the laser power is 1200W (between 3.47 and 1.91 times) over 1300W (between 3.72 and 1.66 times) used of about 45% and 52%, respectively, for worn-out tools. This may be noted that the high temperatures, pressure and cutting speeds applied to the cutting edge during LAT result in damage and flaking of the tool coating. Forces variations for worn CM inserts are larger than those observed for LAT. This may be due to the lower uncut chip thickness with CM and enhanced influence of the damaged cutting edge on the cutting forces. So, in this study, LAT

outperforms over CM for P1-P16 by 2.10–0.84 times for fresh tools and 1.36-1.06 times for worn tools at cutting speed of 60–150 m/min with an elevated preheating temperature up to 860°C.

Surface roughness analysis

The change in surface roughness as a function of tool wear progression at 0.05 mm/rev feed rate is shown in Fig. 2(a). From graphs shown, it is clear that the coated carbide tools under LAT conditions generate the lowest roughness. However, surface roughness shoots more rapidly when tool wear rises. The experimentation is carried out under laser power 0 W, 1200W, 1300W, respectively. The magnitude of arithmetic average surface roughness Ra is about 0.2587-0.5462 µm and 0.3358- 0.6328 µm by LAT when laser power is 1200 W and 1300 W, respectively for fresh cutting edge, while it is 0.4169- 0.8143 µm in conventional machining at feed rate of 0.05 mm/rev as well as cutting speed from 60-150 m/min. For instance, as the laser power is increased from 1200 W to 1300 W, the improvement of surface roughness by LAT is 1.61 times (i.e. from 0.4169 µm in CM to 0.2587 µm in LAT), at cutting condition (P1) is decreased to 1.28 times (i.e. from 0.8143 µm in CM to 0.6328 µm in LAT) at cutting condition (P12) than conventional machining. An increment in laser power led to increased tool wear that consequently upsurges surface roughness. Increasing cutting speed at low feed rate led to decrease in the temperature at tool/chip interface which therefore promoted tool wear, hence increased surface coarsening in LAT. Before the cutting edge is severely worn (flank wear, Vba, value reaches 0.3 mm, as per ISO 3685), the Ra roughness stays as low 1.026-1.247 µm and 1.465–1.778 µm by LAT when the laser power is 1200 W and 1300 W, respectively. In comparison with CM, surface finish gets worsened rapidly at 1.931-2.170 µm with a feed rate of 0.05 mm/rev as well as an increase in cutting speed from 60-150 m/min. Surface finish increases at the end of tool life criteria as a result of the rise in

cutting speed due to BUE formation (adhered layer on rake surface) and/or which can be described by either the possibility of chatters due to vibrations or material plasticity related to high cutting speeds. For example, when comparing cutting condition P1 with P9, the surface roughness is 1.026 µm and 1.465 µm at a laser power of 1200 W and 1300 W during which the machining length lasts for about 250 mm and 180 mm length while in CM it is 1.931 µm when machining length lasts for about 150 mm. On comparing with conventional machining, surface roughness in LAT is improved by 46% to 1200 W and 23% for 1300 W, respectively. In another example, for comparing the cutting condition of P4 with P12, the improvement in surface roughness is 10% for 1200 W and 7% for 1300 W, respectively. In LAT, a decrease in speed, as well as feed, led to an increase in interface time between source and workpiece which resulted in less flank wear. It also restricted the formation of BUE formation, chatters and sufficient material softening due to controlled laser power being in use.

The changes in surface roughness as a task of flank wear progression at feed rate 0.125 mm/rev is shown in Fig. 2(b). During LAT process, the magnitude of roughness has a decreasing trend when compared with conventional machining even at a higher feed rate of 0.125 mm/rev involving both fresh tools as well as a worn-out tool. This signifies that material removal is supported through the increase of temperature using the laser power of 1300 W. Therefore, the tool was less thermally loaded and thus surface roughness is improved. Moreover increasing feed rate resulted in increasing flank wear due to increased friction between chip/tool interfaces, thus an improvement in surface roughness is decreased. For example, on comparing cutting condition of P8 with P16, the surface roughness is found to be 1.182 µm after machining a 130 mm length at a laser power of 1200 W and 1.25 µm at a laser power of 1300 W after machining a 140 mm length. In CM, the surface roughness is found to be 1.75 µm after machining of 110 mm. From the comparison of conventional machining, the surface roughness in LAT is extended by 32% for 1200 W and 28% for 1300

W, respectively. In another example, on comparing the cutting condition of P6 with P14, the improvement in surface roughness is 7% for 1200 W and 4% for 1300 W, respectively.

Through experimental results, it can be observed that surface roughness and tool wear via LAT is consistently lesser than that of CM for speed up to 150 m/min displayed in Fig. 2 (a) and Fig. 2(b), respectively. It can be concluded that LAT outperforms CM by 2.15–0.10 times at speeds of 60–150 m/min at the initial cut of 50 mm. In the length of cut of 200 mm, the improvement by LAT is approximately 1.53-1.02 times at speeds of 60-120 m/min with conventional machining. But for high cutting speeds, the length of cut is reduced to 150 mm. However; LAT results in 1.26 times when compared to CM. The percentage reduction in surface roughness for trial P1-P16 is depicted in Fig. 2(c). The improvement in surface roughness is noticed for about 46% - 32% at speeds of 60–150 m/min for 1200 W laser power and for about 23% - 28% at speeds of 60–150 m/min for 1300 W laser power.

Tool wear analysis

Tool wear analyses are carried out with laser assistance for the cutting conditions (P1-P16) as tabulated in Tables 1 and 2, respectively. For comparison purpose, the progression of tool wear is measured under conventional (CM) machining conditions without laser power. The tool life rejection criteria for both CM and LAT are in employment based on flank wear, crater wear and the edge of chipping or tool fracture. In the present study, the tool life (maximum permissible machining length) is planned from the flank wear. For each machining trials (P1-P16), fresh cutting tools are used, the progression of wear curve is recorded for every 50 mm length and experiments are conducted until tool life criteria (Vba) reaches 0.30 mm. Average measured flank wear (Vba) based on machining length is shown in Figs.3(a-h), respectively. The values of flank wear increase for both LAT and CM with machining length. On the contrary, the progression of the tool flank wear curve is different

for both LAT and CM. Three different stages are observed in the wear curves. The obtained experiment results are agreed [31, 32].

From experimental results, it is observed that the slope of wear curve in CM is larger than the LAT. This implies that rate of wear curve is more rapid in CM for initial wear stage for all the cutting conditions. In steady wear stage, the period of wear is very short. But the wear rate increases remarkably in rapid wear stage than the other two stages. The wear curves observed with LAT that refer to the flank wear versus the machining length is divided into three disparate zones being shown in Figs. 3(a-h), respectively. In the first region, wear rate is somewhat on the higher side because of damaged tool layers at the time of machining and then becomes relatively constant. The second region of steady-state wear in which uniform wear noticed that remained constant till tool failure criteria has been reached. Under the tested cutting conditions of LAT, the generated cutting temperature (≈860°C measured in the primary cutting zone using an infrared pyrometer resulted in a decrease of the yield strength and work hardening) is controlled by laser power and the temperature is dispersed uniformly on tool rake face. This might be a reason for uniform tool wear on flank face. In the third region of wear curve, because of increased magnitude of forces as well as cutting temperatures, the tool flank wear rate has been accelerated and there is no obvious transition of wear curve from second to the third region. This implies that flank wear land has increased with progression of machining length.

For comparative analysis, the progression of tool wear is drawn for cutting conditions P1-P16 under laser power 0W, 1200W and 1300W, respectively. The results are plotted and shown in Figs. 3(a-h), respectively. The magnitude of flank wear is about 0.042-0.089 mm and 0.072 - 0.154 mm by LAT when the laser power is 1200 W and 1300 W, respectively for few cutting edges, while it is 0.082 - 0.178 mm µm in conventional machining at feed of 0.05

mm/rev and speed from 60-150 m/min. For instance, when laser power is increased from 1200 W to 1300 W, the improvement of flank wear by LAT is 23% (i.e. starting 0.178 mm in CM to 0.136 mm in LAT), at cutting condition (P8) is lessened by 13% (i.e. starting 0.178 mm in CM to 0.154 mm in LAT) at cutting condition (P16) than conventional machining. This is due to the fact that the interaction between workpiece-tool interfaces is shorter that can result in low absorption of temperature on being very close to tool flank cutting edge. The increase of speed and feed result in greater tool flank wear, consequently thus the length of cut are decreased. For example, the flank wear reaches tool life criteria of 0.3 mm (ISO 3685) only after machining length of 250 mm for 60 m/min having feed rate of 0.05 mm/rev at 1200 W (P1) and machining length of 120 mm for 150 m/min with 0.125 mm/rev at 1300 W (P16), respectively. In CM, tool wear is found to be 0.302 mm and 0.328 mm when machining length survives about 150 mm for P1 and about 110 mm for P16. In comparison to that of conventional machining, the carbide tool life in LAT is extended by 66% for 1200W (P1) and 8% for 1300W (P16), respectively.

In initial stage for all cutting conditions, wear mechanism in LAT is smooth abrasive wear (marks parallel sloping to the cutting speed direction) on tool rake as well as flank. This is because of a hard constituent part like nitride, carbon; and oxide compounds being present. Additionally, during LAT of Inconel 718 using PVD (AlTiN) tool, in addition to all tests grooves (parallel marks) are sloping along the cutting direction on tool flank surface which has been perceived. This seems to be the results of high abrasive wear. With LAT, the hard particles in microstructure get softened to a point which resulted in less abrasion compared to CM. Grooves usually appear at the beginning of the machining and are never wiped out and this is in good agreement with the other conveyed literature [33, 34]. According to these figures on tool rake and flank, further cutting resulted in coating flaking being observed in Figs. 3(a-h). This is because of crack initiation at the interface between coating and substrate.

No adhesion is observed on cutting edge and rake face of cutting tool. Crater wear and edge chipping are not observed in Figs. 3(a-h). This indicates that the tools used for all operating conditions are having wear resistance in LAT than CM on the basis of tool life. In LAT, aluminum oxide coatings withstand the high cutting temperatures and the cutting tool experiences lower mechanical stresses at interfacial regions. It is also perceived that the coarsening of the surface is minimized. Thus, removal of coating, as well as mild cracking over the tool flank face, parallel to cutting direction has been realized.

In CM, main tool wear mechanism in initial stage of CM for all the cutting conditions is abrasion and adhesion wear on tool rake and flank of cutting tool. The presence of provoked failure of edge breaking from rake face of the cutting tool and non-uniform flank wear resulted in higher tool wear in CM. This is attributed to the fact that aluminum oxide coating on the AlTiN is exposed at low cutting temperatures which result in increased tool wear. As the length of cut continues, excessive chipping along with edge breakage along cutting edge for all the cutting conditions results is observed. The provoked failure is due to large mechanical stress owing to intermittent machining as well as the high cutting temperature at environs of cutting edge. The contact area between tool and chip interfacial regions has been reduced significantly at high cutting speed. This resulted in the reduction of strength of cutting edge and sharp increases in wear rates at higher cutting speed.

The above discussion indicated that the magnitude of flank wears increases with the rise in cutting speed along with feed rate for LAT and CM. However, a sharp reduction in flank wear is observed in all tested cutting conditions when the laser heating is in use. In CM, increased speed along with feed cause greater stress concentration (high temperature) to occur on the tool tip of cutting edge. But, in LAT, the generated cutting temperature in the primary cutting zone has been controlled through laser power and it is more uniformly

dispersed on rake face of the cutting tool. Such outcome results in more uniform flank wear on cutting flank. There is a sign of catering or excess wear on rake face during CM. Also in the microstructure, the presence of hard secondary phases increases the tool wear due to abrasion at conventional cutting temperature. Using LAT, hard particles in microstructure get softened to a point which resulted in lower abrasion. Laser assisted machining at 1200W led to the longest tool life of given tests. Results indicated that LAT with 1200W presented a critical balance through optimization of the laser machining variable along with laser power. Approximately 860°C, Refer Fig. 3(i), is the optimum cutting temperature that allows for the deformation mechanisms of Inconel 718 under high temperature and high strain rate. Suggestions are: (i) Due to the controlled localized heat concentration, suppressing of smearing of hard particle, effectively minimizes the chances of material contact between hard carbide particles and cutting tool; thus, this promotes tool flank wear resistance, (ii) Softness of hard carbide particles with laser assistance propagates occurrence of unfastened abrasive particles which is beneficial to cutting tool and finished machined surface (leads to suppressing the surface coarsening). This suggests that the cutting tool has more wear resistance in LAT that of CM based on the calculated tool life.

Thus, it can be concluded from the experimental study that LAT outperforms conventional machining by 2.19–1.05 times at speeds of 60–150 m/min at the initial cut of 50 mm. In the length of cut of 200 mm, the improvement by LAT is approximately 1.53-1.02 times at speeds ranges 60-120 m/min with conventional machining. But for high cutting speed, the length of cut is reduced to 150 mm. However; LAT results in 1.05 times than CM. The progression of tool wear for trial P1-P16 is depicted in Fig. 3(j). It is noticed that improvement in tool life is about 66 % - 8% at speeds of 60–150 m/min for laser power of 1200 W and about 30 % - 8% at speeds of 60–150 m/min for laser power of 1300 W.

Tool failure mode analysis

To understand the modes of tool failure under CM and LAT; failed tool is analyzed under scanning electron microscope (SEM). SEM images of the tool flank for cutting conditions P1, P9, P8, P16, P4, P12, P5, P13 for laser assistance and C1, C8, C4, C5 for conventional machining are shown in Fig. 4(a). For all the tested coated carbide tools, for both the machining, dominating tool wear mechanism is average flank wear on flank face. In addition to average flank wear, tool material is worn out, chipping of the cutting edge and flanking of coating (C1) is observed at the tool nose radius corner for CM. The rise of speed at the low feed (C4), abrasion as well as adhesion on the flank face of cutting edge is observed. The result of tool material edge chipping is likely due to that of strong cyclic (vibration) impacts. Abrasion primarily occurs because of hard precipitates and particles of workpiece material. Adhesion is mostly caused by high temperatures and pressure during the machining process. As a result, welding is done between the fresh surface of chip and rake face. As well, similar observations are found for the rise of feed rate from 0.05- 0.125 mm/rev for cutting conditions C5 and C8. From SEM analysis of C5 and C8, evidence of carter wear has been found because of diffusion wear mechanism. Due to excessive generation of heat and close physical contact of the workpiece with the tool, a result of machining at high cutting speeds, accelerated diffusion process and thus crater wear was formed on rake face of the cutting tool.

An EDS detector has been used to examine tool in worn out region i.e., regions ‘B’ in Fig. 4(b). It can be seen that the elements such as Ni and Cr at region ‘B’ are shown by EDS analyses. The chipping of the tool flank confirmed the presence of tungsten (W) and carbon (C) peaks from region marked “B” in Fig. 4(b). Also flaking is evident from this EDS analysis as elements of the coating such as Ti, Al appears in smaller quantities. It is observed

from the reported tested conditions that, during LAT, the main wear mechanism observed is abrasion a well as flaking of tool coating on tool flank face from SEM images, (i.e. region 'A' in Fig. 4(b), region 'C' in Fig. 4(b). High temperatures applied to cutting edge during LAT resulted in damage and flaking of the tool coating. Without the protective layers, the cutting edge is prone to breaking rather than wearing under such high pressure, temperatures and cutting speeds. Bhatt [35] performed tool life study for the PVD coated carbide AlTiN at 100 m/min and 0.125 mm/rev under CM conditions. The author observed severe crater wear on rake face because of hard workpiece particles causing an abrasive action on the rake face at high temperatures, i.e., abrasion, as well as diffusion as a result of high temperatures [35]. Under LAT conditions the thermal softening reduces this phenomenon and no crater wear is observed. It can be seen that the smaller quantities of elements such as Ni and Cr at region 'A', 'B', 'C', 'D', 'E', 'F' are shown by EDS analyses. The other modes of failure such as adhesion, tool edge chipping, and built-up-layer are not evident from the SEM images. This can be possible due to the fact that, during LAT, the strength of cutting tool is not weakened under high cutting temperature. In other words, the material tensile strength of Inconel 718 drastically decreases; thus, the forces are significantly reduced even at high speed and feed. The titanium-based hard coating possesses appreciable oxidation resistance; considerable chemical stability at elevated temperature; increased hot hardness; and low heat transfer coefficient during machining of Inconel 718.Moreover, fine-grained K5525 grade of WC substrate with 10% binder, offer superior deformation resistance.

Surface integrity analysis

The surface and subsurface topography of Inconel 718 machined sample under CM and LAT are investigated using an optical microscope. These are obtained by cross-sectioning the cylindrical workpiece at the end of tool life for LAT and CM. These specimens

are prepared by sectioning with an abrasive cut-off wheel, Bakelite mounting, grinding and polishing with alumina particles and then chemically etching with Picral's reagent. Grain size is a vital microstructural parameter. Here, the grain size is measured on digitally recorded optical images for P1-P16 and C1–C8, as shown in Figs 5(a-d), respectively to find the effect of LAT on final part microstructure. Comparative study of grain size and orientation is performed for both the surface and subsurface for two laser power. For subsurface analysis, average grain size of about 45 μm,30 μm along with 35 μm are measured for CM, 1200 W and 1300 W, while for surface topography 40 μm, 25 μm and 30 μm for CM, 1200 W and 1300 W for all the cutting conditions. Using LAT, since heat affected zone is effectively removed, no sign of change in phase transformation, the formation of the white layer and any other defects in the microstructure of the machined part has been observed. The grains formed by LAT adjacent to the machined surface are little and evenly spread when compared to original unaffected area. Grain orientation was observed to be random, having no specific orientation resulting under LAT. As a whole, no substantial difference is observed between CM and LAT when examined optically by comparing the microstructures of cross-sections of machined samples.

Chip morphology

The type of chips produced during machining is determined by the cumulative effects of cutting methods, i.e. continuous/intermittent, the material being cut, tool geometry, cutting conditions, cutting fluid type and its application method, etc. The chip produced during initial and final cut i.e. when the tool is worn out is recorded under an optical microscope. At low cutting speed, shorter irregular chips are formed. At initial cutting condition with low cutting speed and feed rate, silver color snarled ribbon chip is formed for CM (C1), golden brown colored snarled helical chip is formed for 1200W (P1) and 1300W (P9) as shown in Fig. 6

(a). Similarly, at the worn out condition, the long washer type helical chip is formed for CM (C1), golden colored long ribbon chip is formed for 1200W (P1) and 1300W (P9)as shown in Fig.6 (b). At initial cutting condition with higher speed and feed silver colored long ribbon chip is formed for CM (C8), bluish violet colored long snarled washer type helical chip for 1200 W (P8) and at laser power 1300W(P16) as shown in Fig. 6(c) golden colored long ribbon chip are formed. Similarly, at worn out condition snarled ribbon chip is formed for CM (C8), golden colored long ribbon chip is formed for 1200W (P8) and the golden colored long washer type helical chip is formed for 1300W(P16) as shown in Fig. 6 (d).

In machining with PVD coated tungsten carbide (P1-P8 conditions), helical tubular and ribbon chip formation was observed for fresh tool and with the continuing machining operation, short and long ribbon chip formation was also observed. Similarly, for machining conditions P9-P16, snarled washer and ribbon chip formation was observed for fresh tool and with the continuing machining operation, short and long tubular chip formation was also observed. Particularly, in the P1 and P5, a ribbon and short chip formation was observed and the highest Ra values were reached in all of the tests as 1.50 µm and 1.88 µm, respectively. Similarly, in the P12 and P13, a long and short washer type helical chip formation was observed and the highest Ra values were reached in all of the tests as 1.77 µm and 2.15 µm, respectively. In the cutting conditions P1, P2 P15 and 16, the chip formation was long ribbon shape. The lowest Ra value is reached at the P1 cutting conditions as 0.6583 µm.

The slipping angle, chip thickness, and tooth-pitch are measured for condition P1 and P9 at different locations using an optical microscope. The values are measured at least on 10 chip cross-section serrations that are sectioned upright to the width of the chip and are presented in Fig. 6(e). The saw-tooth formation of the chip is observed for both CM and LAT. On the contrary, in LAT process, the division of saw-tooth chip has been increased

when compared to that of CM which evidently revealed the thermal softening effect. For example from Fig.6 (e), the slipping angle of the segmented chip was about 50.6º for LAT (compared from 53.75º in CM) under the laser power of 1200W and 50.2º for LAT at the laser power of 1300W when the length of cut is 50 mm. However, the slipping angle gradually decreased when the length of cut increased. The maximum chip thickness (h_{max}) of the segmented chip is about 96.89 µm for LAT under laser power 1200W and 106.77 µm for LAT under laser power 1300W (compared from 112.7 µm in CM) when the length of cut is 50 mm. Similarly, the minimum chip thickness (h_{max}) was 64.15 µm for LAT under laser power 1200W and 65.68 µm for LAT under laser power 1300W (compared from 78.64 µm in CM) at the end of tool life. The distance between sawtooth chips is about 29.21 µm for LAT under laser power 1200W and 32.51 µm for laser power 1300W (from 38.66 µm in CM) at the length of cut of 50 mm which increases when the length of cut is increased. From chip analysis, decreased shear angle is also observed and thus leads to the increase of uncut chip thickness (h_{max}) in LAT. These changes in the shear angle and the distance generate an increased frequency of segmentation of the chip. The rise in laser power increased the shear angle and reduced with increment in feed rate in LAT. This resulted in the decrease in cutting force, surface roughness and tool wear during LAT. Moreover, it is observed that amount of chip curvature reduced for every test conducted under LAT when compared to that of CM. Change in chip color is also observed due to a high surface temperature in LAT.

Conclusion

This research work examined the influence of operating parameters on machinability characteristics on Inconel 718 with carbide inserts. Force, surface roughness, tool life, as well as subsurface damage have significantly reduced under LAT when compared to that of CM. 1200 W is established as the optimum laser power even at a higher feed of 0.125 mm/rev,

cutting depth of 0.5 mm, and speed of 150 m/min with carbide tooling. Employing this laser power, LAT provides 2.10 times decrease in cutting force, 46% reduction in the surface roughness along with 66% improvement in tool life on analysis that of CM by using the flank wear (300 μm) as a metric in order to recognize effective tool life. Compared to CM, with the application of laser the cutting speed of carbide tool is increased to an ideal cutting condition of 150 m/min, 0.125 mm/rev without subsurface damage. This can be due to the preheating temperature along with heat affected depth for material using a laser source that is effectively controlled under the various combinations of laser machining parameters. This reduction has been further analyzed by geometrical characteristics of the chip. The saw-tooth chip produces maximum undeformed chip thickness of about 98.96 μm in LAT. In chip formation, the increment in chip thickness, reduction in shear angle and decrement in saw-tooth pitch is also noticed in LAT as compared with that of CM. The investigations on tool wear mechanism reveal the presence of abrasion, flaking, catering and edge chipping for CM while abrasion and flaking for LAT. This means that LAT relieves the strong surface work hardening effect induced by machining. From surface and subsurface analysis, phase transformation change, the formation of the white layer and any other defects under LAT is not noticed. This may be attributed to the fact that there is no change in the hardness value (48 HRC) of the machined surface due to laser heating. This indicates that LAT parts present better surface integrity that of CM machined parts. Further, the scope is extending to study the mechanical properties of LAT turned parts for the determined laser assisted cutting conditions. Finally, economic analysis of the LAT process is also the scope of the present research.

Acknowledgement

The authors acknowledge the Department of Science and Technology, India and VIT University for funding the Laser facilities at Centre for Advanced Materials Processing and Testing Lab, under DST-FIST scheme (Grant No: SR/FST/ETI- 282/2010C). The authors

also acknowledge Dr. P. Kuppan, Professor, School of Mechanical Engineering, for valuable support for the experiments.

References

[1] Ezugwu EO. Key improvements in the machining of difficult-to-cut aerospace superalloys. Int J Mach Tool Manu 2005;45(12):1353-67.

[2] Venkatesan K, Ramanujam R, Kuppan P. Laser assisted machining of difficult to cut materials: research opportunities and future directions-a comprehensive review. Procedia Eng. 2014; 97:1626-1636.

[3] Kannan V, Radhakrishnan R, Palaniyandi K. A review on conventional and laser assisted machining of aluminium based metal matrix composites. Engineering Review. 2014 4;34(2):75-84.

[4] Costes JP, Guillet Y, Poulachon G, Dessoly M. Tool-life and wear mechanisms of CBN tools in machining of Inconel 718. Int J Mach Tool Manu 2007; 47(7):1081-7.

[5] Bushlya V, Zhou J, Ståhl JE. Effect of cutting conditions on machinability of superalloy Inconel 718 during high speed turning with coated and uncoated PCBN tools. Procedia CIRP 2012;3:370-5.

[6] Jemielniak K. Finish turning of Inconel 718. Advanc Manuf Sc Techn 2009; 33(1):59-69.

[7] Arunachalam RM, Mannan MA, Spowage AC. Surface integrity when machining age hardened Inconel 718 with coated carbide cutting tools. Int J Mach Tool Manu 2004;44(14):1481-91.

[8] Coelho RT, Silva LR, Braghini A, Bezerra AA. Some effects of cutting edge preparation and geometric modifications when turning INCONEL 718™ at high cutting speeds. J Mater Process Tech 2004; 148(1):147-53.

[9] Prengel HG, Pfouts WR, Santhanam AT. State of the art in hard coatings for carbide cutting tools. Surf Coat Tech 1998; 102(3):183-90.

[10] Thakur A, Gangopadhyay S. State-of-the-art in surface integrity in machining of nickel-based super alloys. Int J Mach Tool Manu 2016; 100:25-54.

[11] Jindal PC, Santhanam AT, Schleinkofer U, Shuster AF. Performance of PVD TiN, TiCN, and TiAlN coated cemented carbide tools in turning. Int J Refract Metals Hard Mater 1999; 17(1):163-70.

[12] Devillez A, Le Coz G, Dominiak S, Dudzinski D. Dry machining of Inconel 718, workpiece surface integrity. J Mater Process Tech 2011; 211(10):1590-8.

[13] Sharman AR, Hughes JI, Ridgway K. Workpiece surface integrity and tool life issues when turning Inconel 718™ nickel based superalloy. Mach Sci Technol 2004;8(3):399-414.

[14] Akhtar W, Sun J, Sun P, Chen W, Saleem Z. Tool wear mechanisms in the machining of Nickel based super-alloys: A review. Front Mech Eng 2014; 9(2):106-19.

[15] Anderson M, Patwa R, Shin YC. Laser-assisted machining of Inconel 718 with an economic analysis. Int J Mach Tool Manu 2006; 46(14):1879-91.

[16] Attia H, Tavakoli S, Vargas R, Thomson V. Laser-assisted high-speed finish turning of superalloy Inconel 718 under dry conditions. CIRP Ann Manuf Techn 2010; 59(1):83-8.

[17] Garcí V, Arriola I, Gonzalo O, Leunda J. Mechanisms involved in the improvement of Inconel 718 machinability by laser assisted machining (LAM). Int J Mach Tool Manu 2013; 74:19-28.

[18] Germain G, Lebrun JL, Braham-Bouchnak T, Bellett D, Auger S. Laser-assisted machining of Inconel 718 with carbide and ceramic inserts. Int J Mater Form 2008; 1(1): 523-526.

[19] Venkatesan K, Ramanujam R, Kuppan P. Parametric modeling and optimization of laser scanning parameters during laser assisted machining of Inconel 718. Opt Laser Technol 2016; 78:10-8.

[20] Venkatesan K, Ramanujam R. Statistical approach for optimization of influencing parameters in laser assisted machining (LAM) of Inconel alloy. Measurement 2016; 89: 97-108.

[21] Venkatesan, K., R. Ramanujam, and P. Kuppan. Analysis of cutting forces and temperature in laser assisted machining of Inconel 718 using Taguchi method. Procedia Eng 2014; 97: 1637-1646.

[22] Venkatesan K, Ramanujam R. Optimisation of machining parameters in laser aided hybrid machining of Inconel 718. Int J of Machining and Machinability of Materials 2016; 18(3):252-72.

[23] Venkatesan K, Ramanujam R. Improvement of Machinability using Laser-Aided Hybrid Machining for Inconel 718 Alloy. Mater Manuf Process 2016; 31(14):1825-35.

[24] Przestacki D, Chwalczuk T, Wojciechowski S. The study on minimum uncut chip thickness and cutting forces during laser-assisted turning of WC/NiCr clad layers. Int J Adv Manuf Tech. 2017:1-2.

[25] Przestacki D, Szymanski P, Wojciechowski S. Formation of surface layer in metal matrix composite A359/20SiCP during laser assisted turning. Compos Part A: Appl Sci Manuf 2016; 91:370-9.

[26] Shokrani A, Dhokia V, Newman ST. Investigation of the effects of cryogenic machining on surface integrity in CNC end milling of Ti–6Al–4V titanium alloy. J Manuf Process 2016; 21:172-179.

[27] Thakur A, Gangopadhyay S. Dry machining of nickel-based super alloy as a sustainable alternative using TiN/TiAlN coated tool. J Clean Prod 2016; 129:256-268.

[28] Pusavec F, Krajnik P, Kopac J. Transitioning to sustainable production–Part I: application on machining technologies. J Clean Prod 2010; 18(2):174-184.

[29] M'Saoubi R, Axinte D, Soo SL, Nobel C, Attia H, Kappmeyer G, Engin S, Sim WM. High performance cutting of advanced aerospace alloys and composite materials. CIRP Ann Manuf Techn 2015; 64(2):557-80.

[30] Rashid RR, Sun S, Wang G, Dargusch MS. The effect of laser power on the machinability of the Ti-6Cr-5Mo-5V-4Al beta titanium alloy during laser assisted machining. Int J Mach Tool Manu 2012; 63:41-3.

[31] Kong X, Zhang H, Yang L, Chi G, Wang Y. Carbide tool wear mechanisms in laser-assisted machining of metal matrix composites. Int J Adv Manuf Tech 2016; 85(1-4):365-79.

[32] Kong X, Yang L, Zhang H, Chi G, Wang Y. Optimization of surface roughness in laser-assisted machining of metal matrix composites using Taguchi method. Int J Adv Manuf Tech 2016; 1-4.

[33] Cantero JL, Díaz-Álvarez J, Miguélez MH, Marín NC. Analysis of tool wear patterns in finishing turning of Inconel 718. Wear. 2013; 297(1):885-94.

[34] Zhu D, Zhang X, Ding H. Tool wear characteristics in machining of nickel-based superalloys. Int J Mach Tool Manu 2013; 64:60-77.

[35] Bhatt A, Attia H, Vargas R, Thomson V. Wear mechanisms of WC coated and uncoated tools in finish turning of Inconel 718. Tribol Int 2010; 43(5):1113-21.

Table 1 Comparative analysis of cutting force (F_z) at 1200W vs 0W

Trial No.	Machining Parameters			Laser Assisted Machining		Conventional machining		Times of improvement	
	cutting speed	feed rate	laser power	Fresh Tool	Worn Tool	Fresh Tool	Worn Tool	Fresh Tool	worn Tool
	m/min	mm/rev	watt	Cutting force (F_z, N)					
P1	60	0.05	1200	71.55	226	105.71	264	1.48	1.17
P2	90	0.05	1200	57.64	189.5	75.8	225.1	1.32	1.19
P3	120	0.05	1200	42.36	146.8	67.92	200.9	1.60	1.37
P4	150	0.05	1200	52.51	132.6	110.2	180.7	2.10	1.36
P5	60	0.125	1200	91.73	275.9	167.2	333.9	1.82	1.21
P6	90	0.125	1200	125.5	239.3	126.6	331	1.01	1.38
P7	120	0.125	1200	85.03	170.8	112.9	194.5	1.33	1.14
P8	150	0.125	1200	96.33	184.5	107.3	225	1.11	1.22

Table 2 comparative analysis of cutting force (Fz) at 1300W vs 0W

Trial No.	Machining Parameters			Laser Assisted Machining		Conventional machining		Times of improvement	
	cutting speed	feed rate	laser power	Fresh Tool	Worn Tool	Fresh Tool	Worn Tool	Fresh Tool	worn Tool
	m/min	mm/rev	watt	Cutting force (F_z, N)					
P9	60	0.05	1300	59.08	204.8	105.71	264	1.79	1.29
P10	90	0.05	1300	81.52	167.2	75.8	225.1	0.93	1.35
P11	120	0.05	1300	64.27	137.8	67.92	200.9	1.06	1.46
P12	150	0.05	1300	63.25	109.9	110.2	180.7	1.74	1.64
P13	60	0.125	1300	110.7	260.4	167.2	333.9	1.51	1.28
P14	90	0.125	1300	121.7	270.3	126.6	331	1.04	1.22
P15	120	0.125	1300	106.6	184.5	112.9	194.5	1.06	1.05
P16	150	0.125	1300	127.6	211.5	107.3	225	0.84	1.06

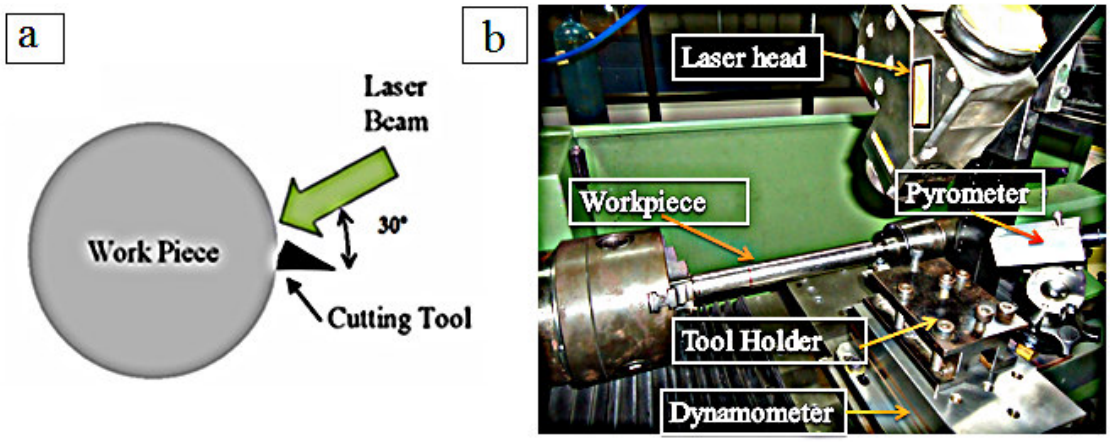

Fig. 1(a) Schematic of experimental setup for LAT

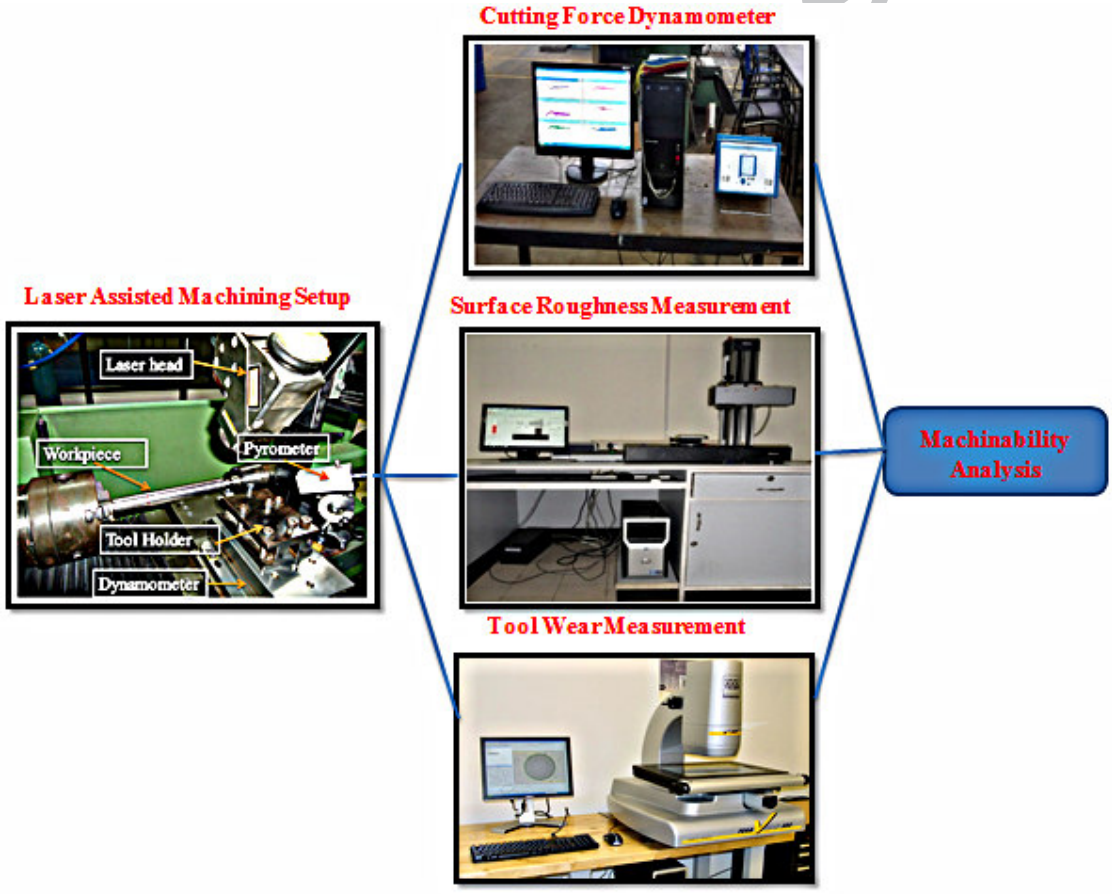

Fig. 1(b) Process flow chart of the experimental step

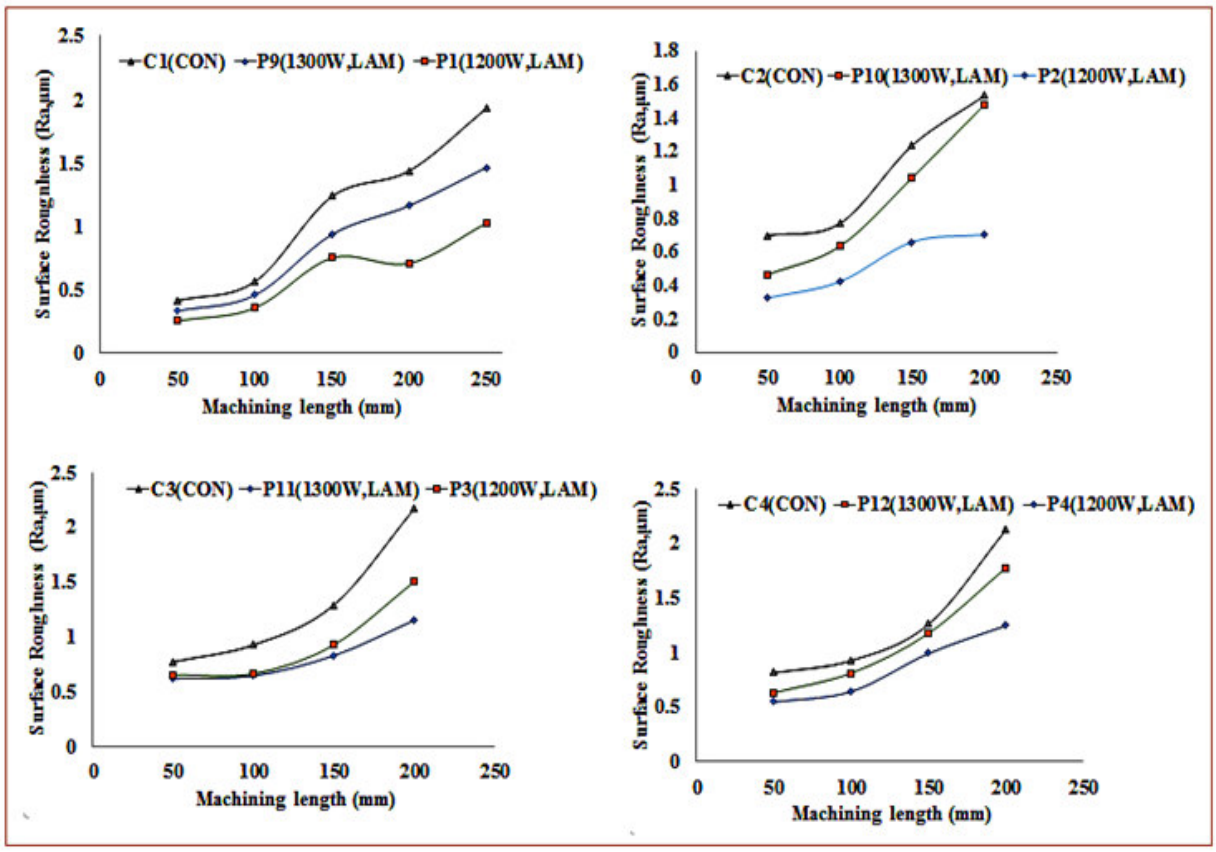

Fig. 2(a) Surface roughness as a function of machined length at feed rate 0.05 mm/rev

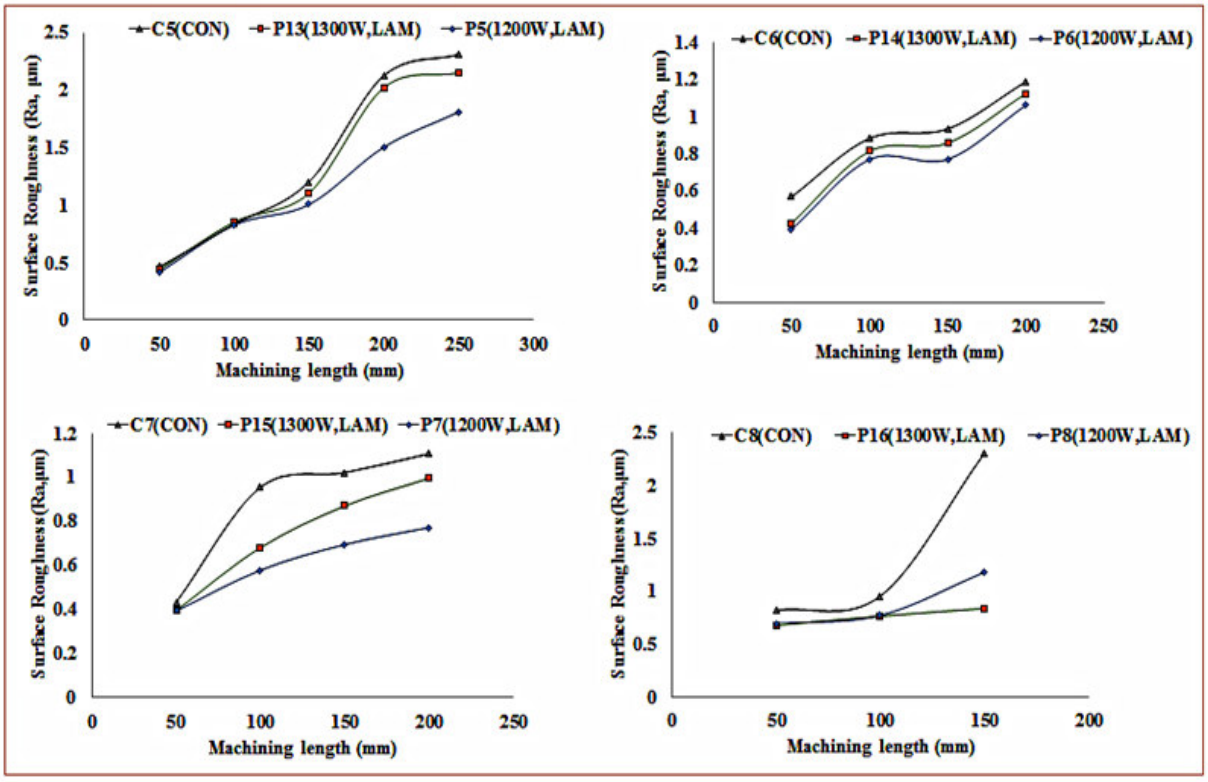

Fig. 2(b) Surface roughness as a function of machining length for feed rate 0.125 mm/rev

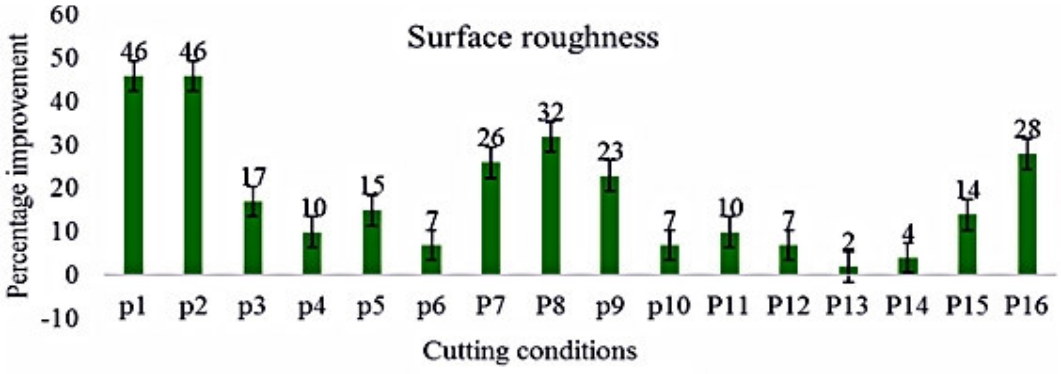

Fig. 2(c) Percentage improvement of surface roughness for cutting conditions P1-P16

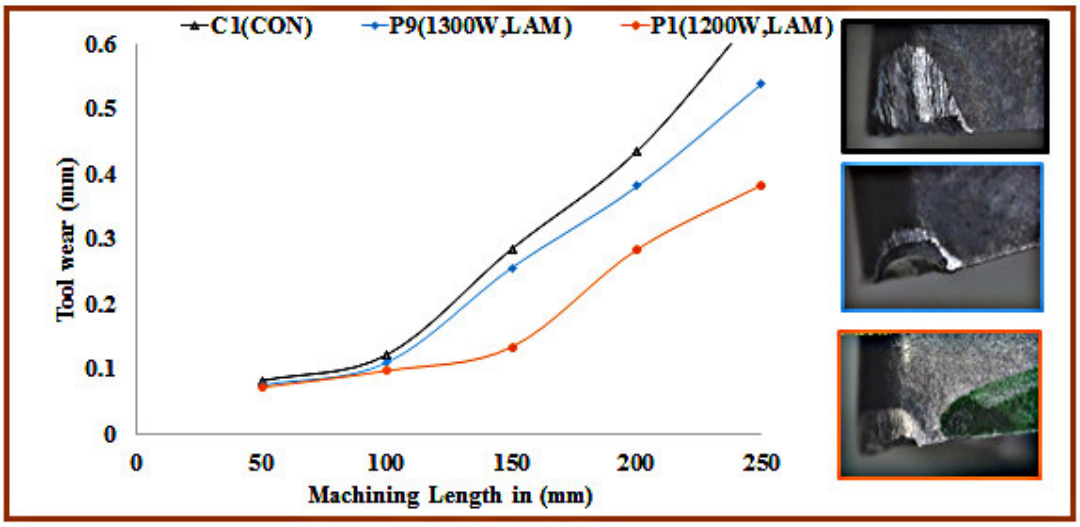

Fig. 3(a) Effect of LAT on flank wear with machining length for trial P1 and P9

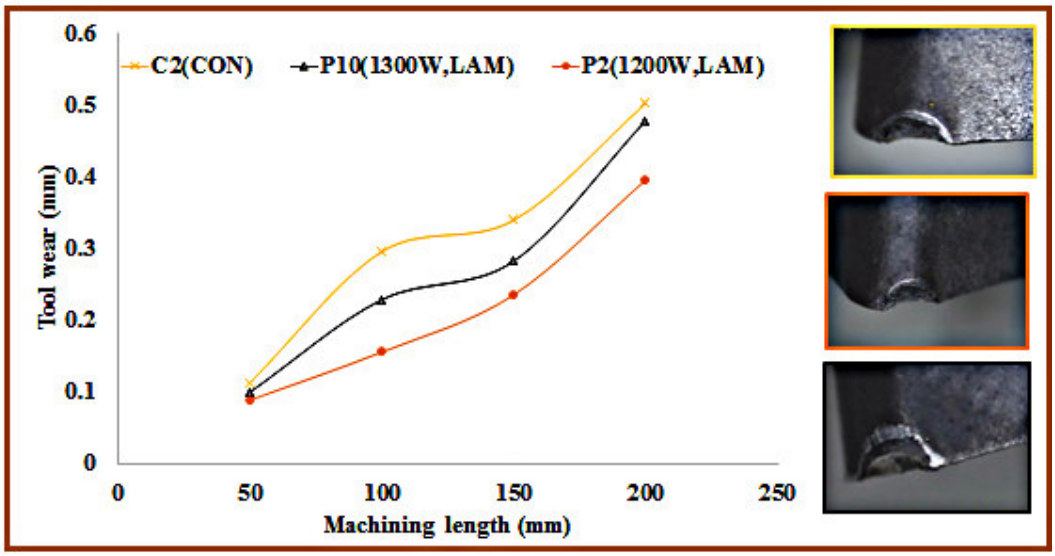

Fig. 3(b) Effect of LAT on flank wear with machining length for trial P2 and P10

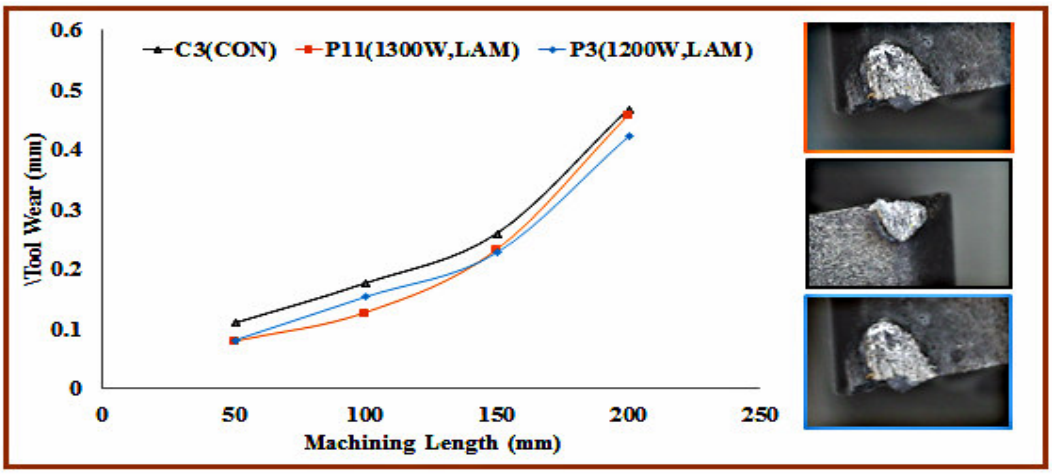

Fig. 3(c) Effect of LAT on flank wear with machining length for trial P3 and P11

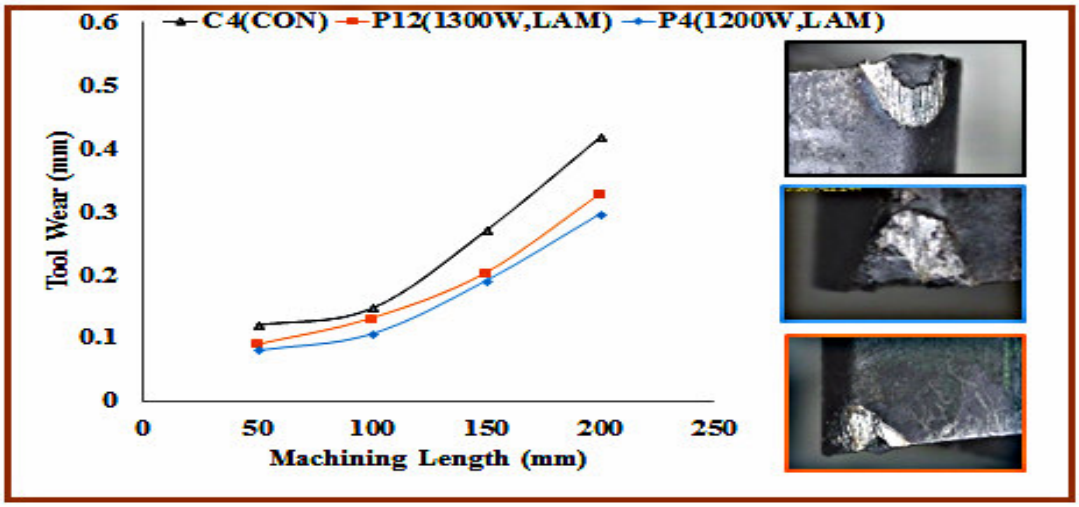

Fig. 3(d) Effect of LAT on flank wear with machining length for trial P4 and P12

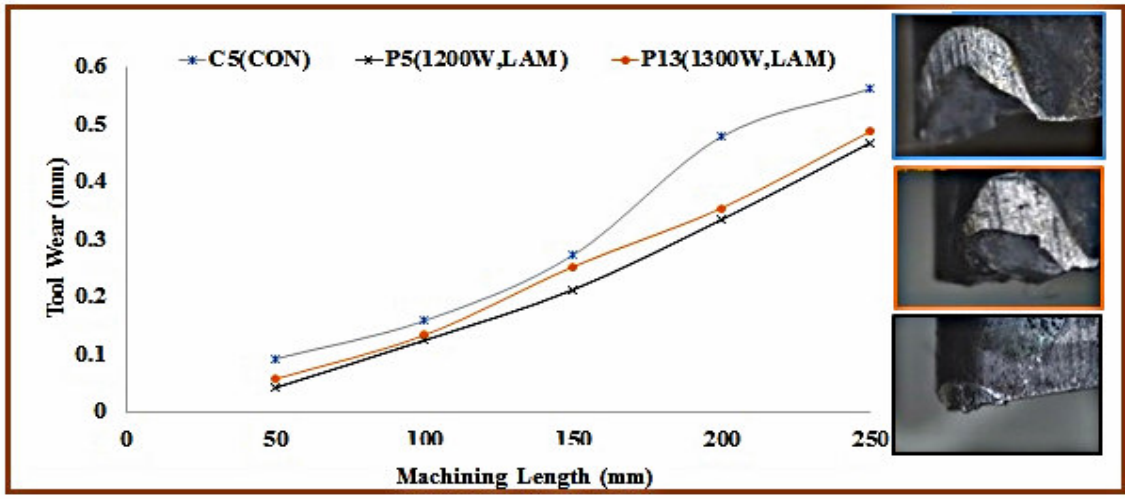

Fig. 3(e)Effect of LAT on flank wear with machining length for trial P5 and P13

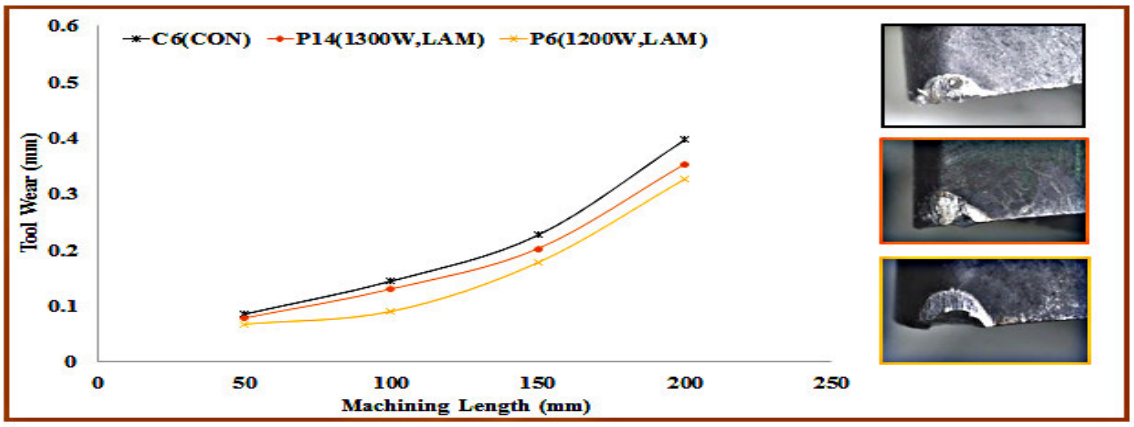

Fig. 3(f) Effect of LAT on flank wear with machining length for trial P6 and P14

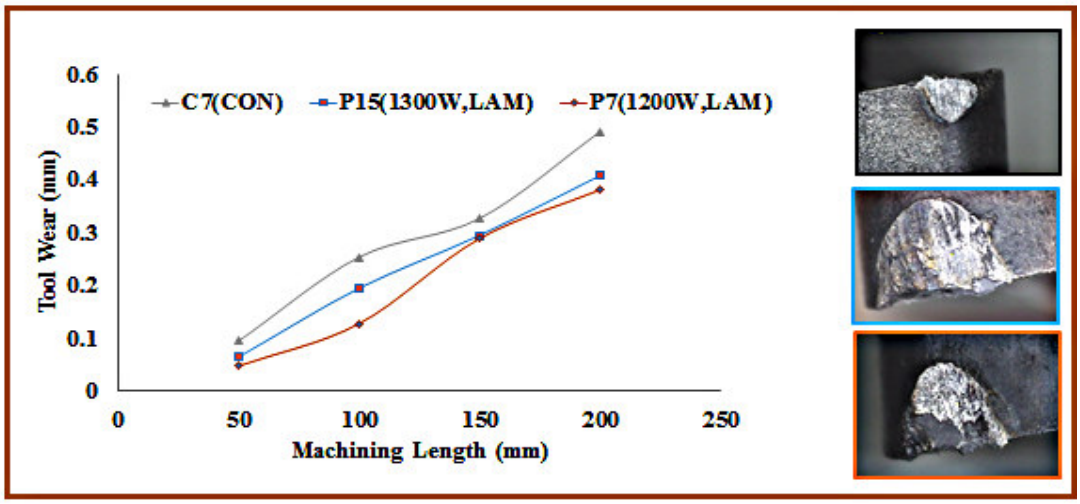

Fig. 3(g) Effect of LAT on flank wear with machining length for trial P7and P15

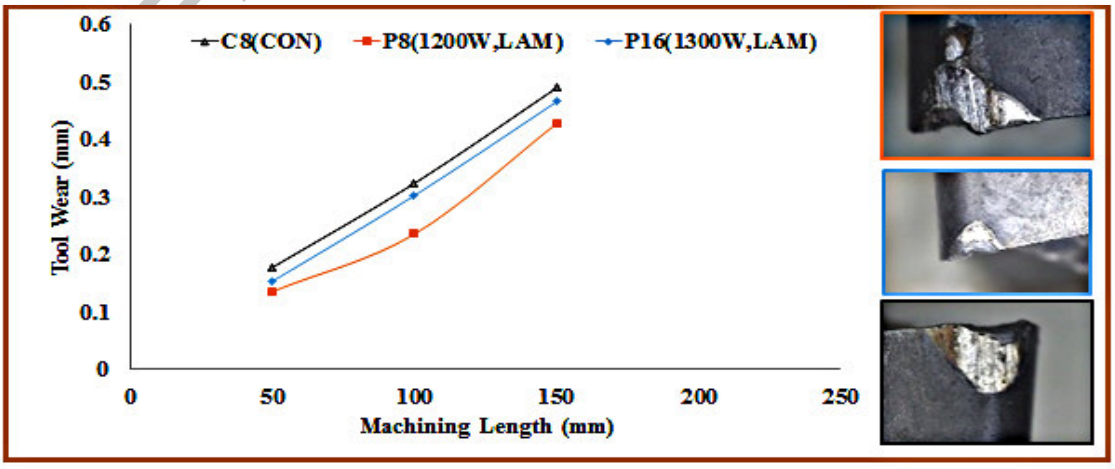

Fig. 3(h) Effect of LAT on flank wear with machining length for trial P8 and P16

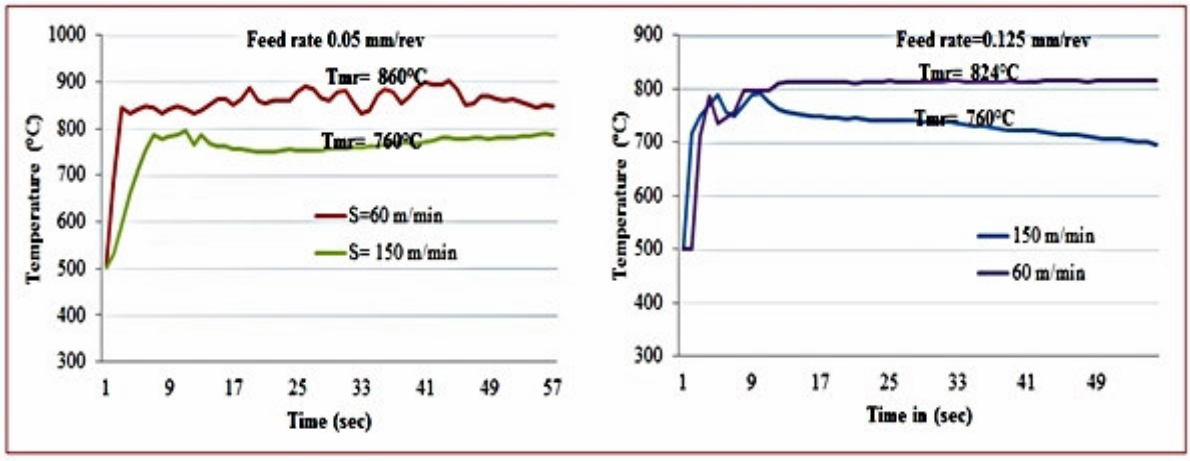

Figure 3(i) Results of surface temperatures f=0.05 mm/rev and P=1200W (a) and f=0.125 mm/rev and P=1300W (b)

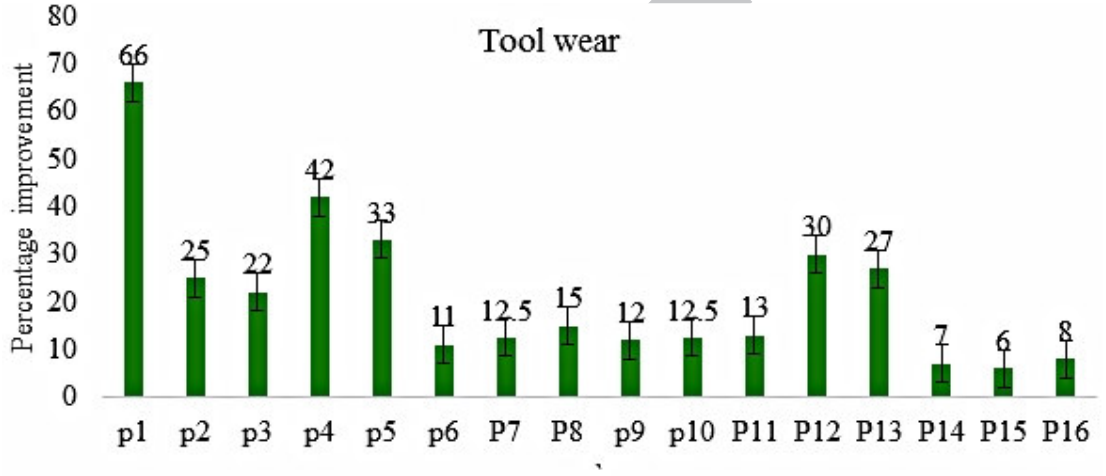

Fig. 3(j) Percentage improvement for cutting conditions P1-P16

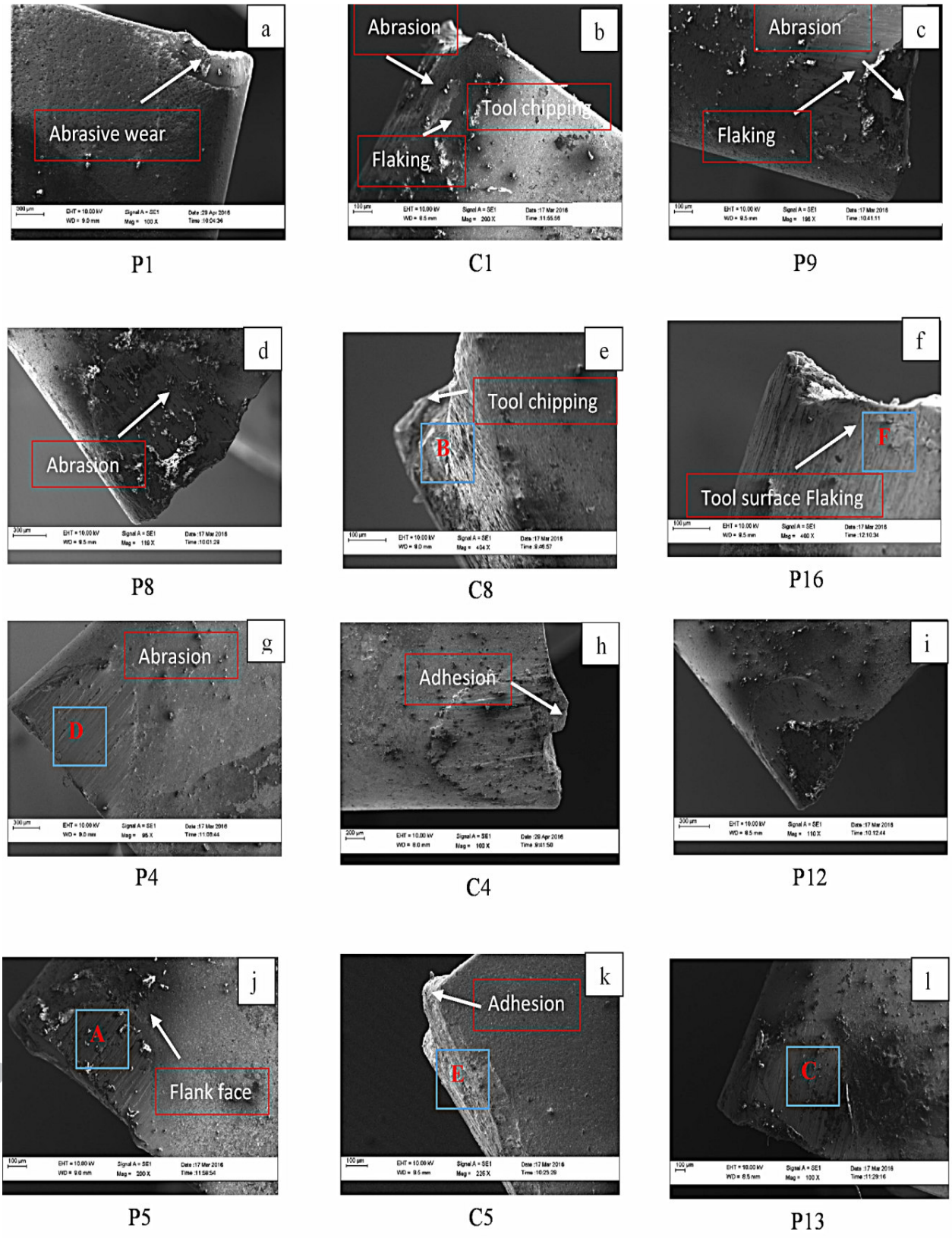

Fig. 4(a) SEM image of failed coated carbide tool in LAT

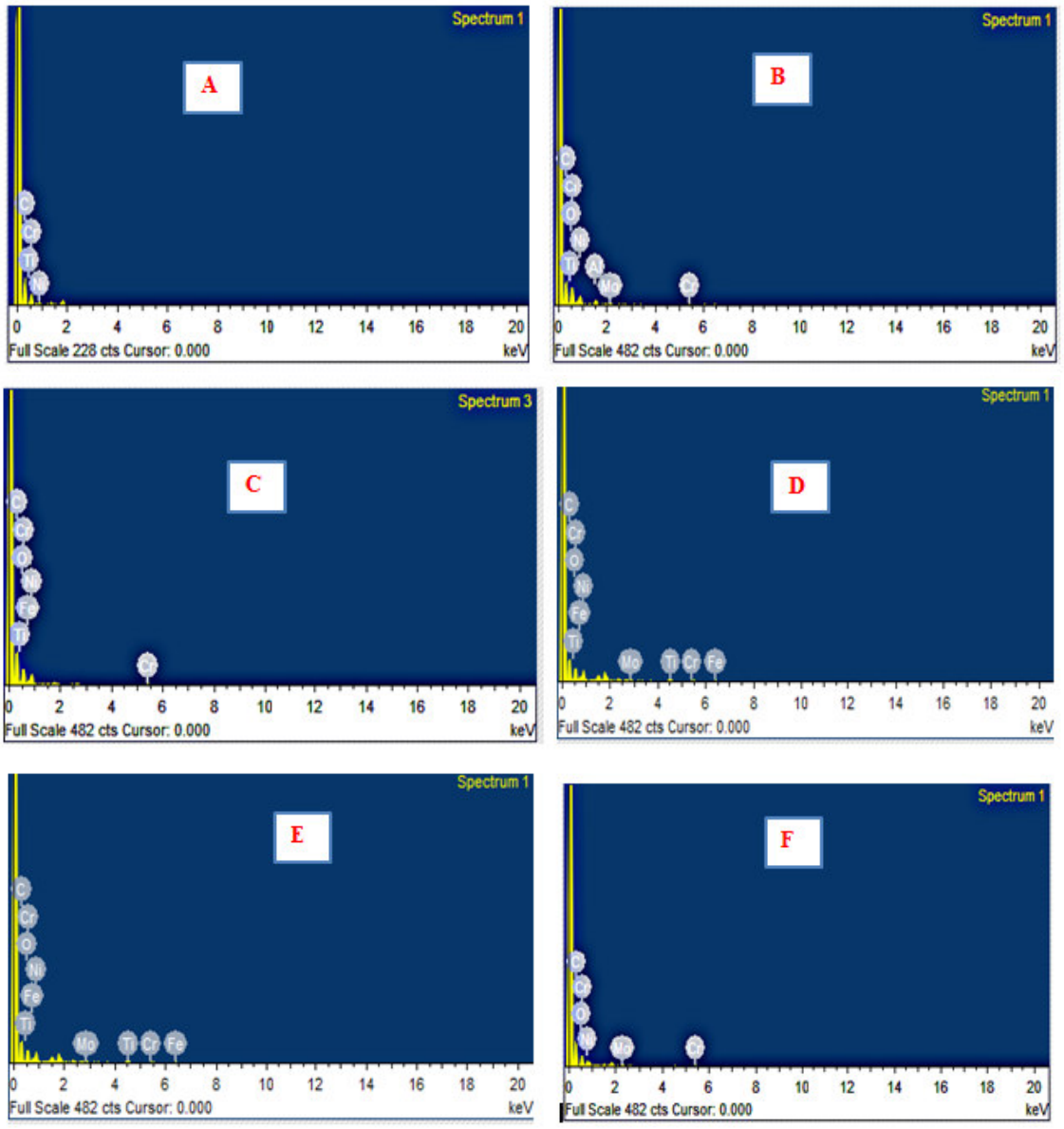

Fig. 4(b) EDS image of failed coated carbide tool

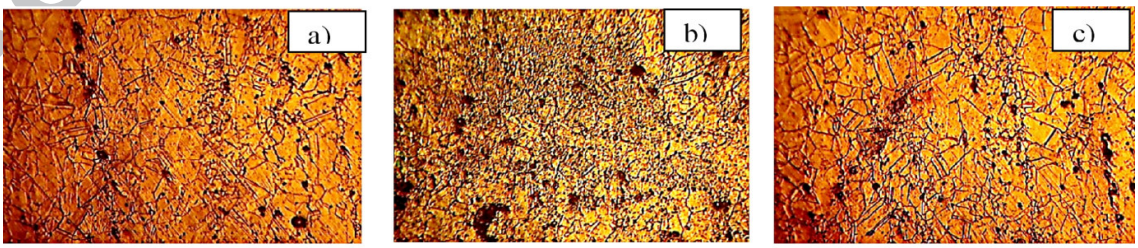

Fig. 5(a) Surface topography for P1 (a), C1 (b), P9 (c)

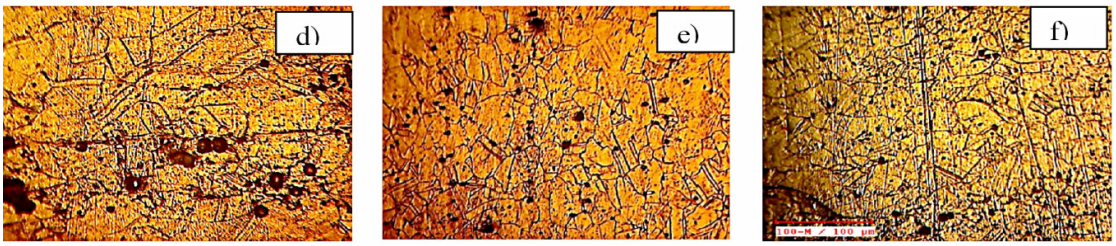

Fig. 5(b) Subsurface topography for P1(d), C1(e), P9(f)

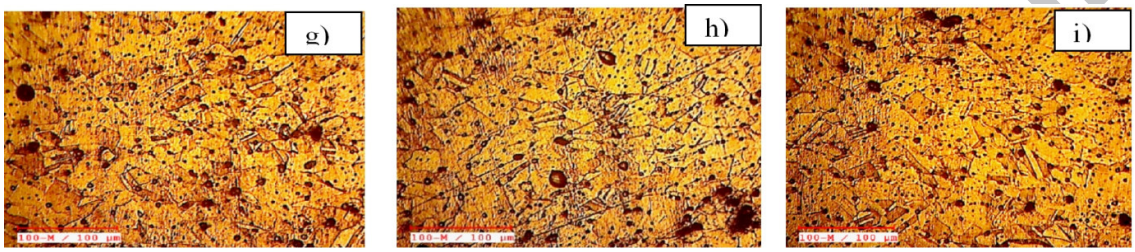

Fig. 5(c) Surface topography P8 (g), C8 (h), P16 (i)

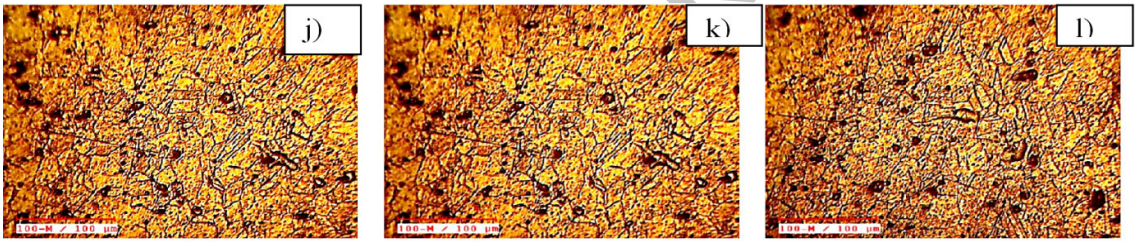

Fig. 5(d) Subsurface topography P8 (j), C8 (k), P16 (l)

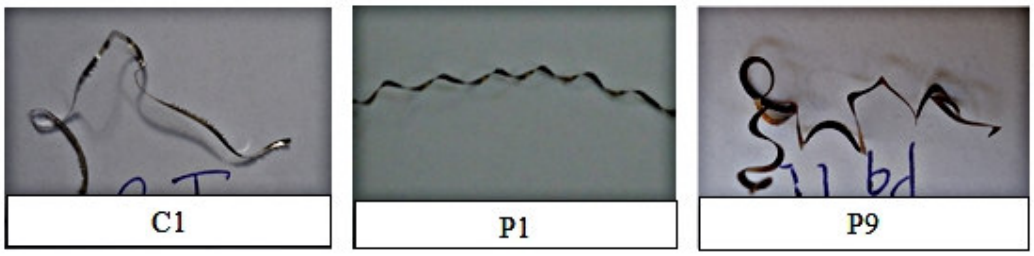

Fig. 6(a) Chip characteristics for C1, P1 and P9 at initial cutting condition

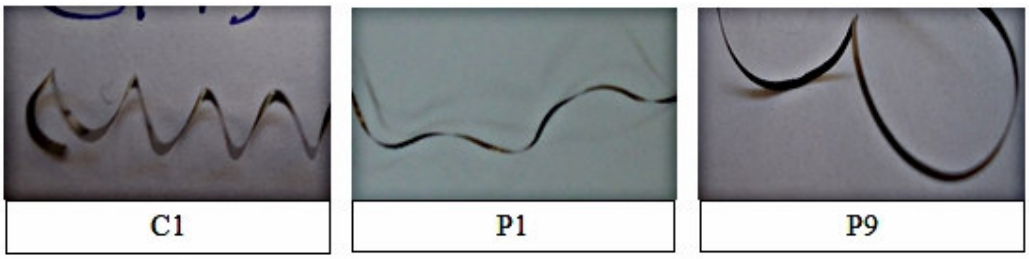

Fig. 6 (b) Chip characteristics C1, P1 and P9 at worn out condition

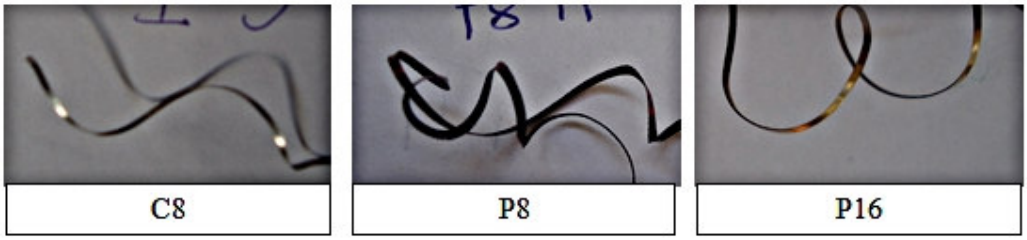

Fig. 6(c) Chip characteristics C8, P8 and P16 at initial cutting condition

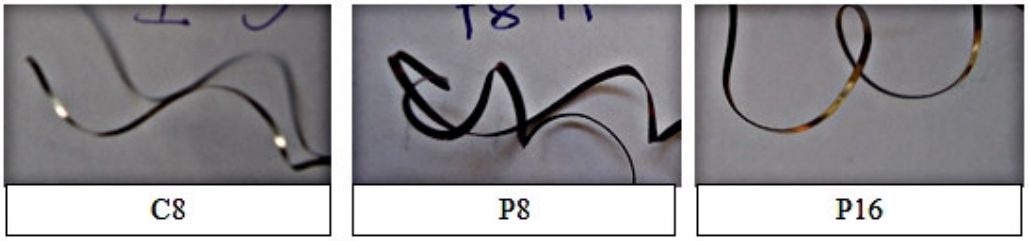

Fig. 6(d) Chip characteristics C8, P8 and P16 at worn out cutting condition

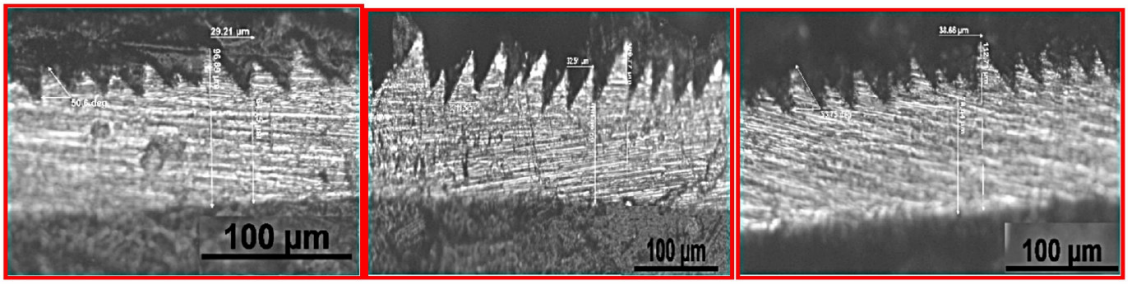

Fig. 6(e) Chip morphology a) LAT (1200W, 0.0 5mm/rev b) LAT (1300W, 0.05mm/rev) c) Conventional machining (0W, 0.05mm/rev)

Conflict of Interest

The authors have declared no conflict of interest

Corresponding author

Dr.K.Venkatesan,
Associate Professor
Department of Design and Automation
School of Mechanical Engineering
VIT University, Vellore, 632014, Tamil Nadu, INDIA

Compliance with Ethics Requirements

This article does not contain any studies with human or animal subjects

Corresponding author

Dr.K.Venkatesan,
Associate Professor
Department of Design and Automation
School of Mechanical Engineering
VIT University, Vellore, 632014, Tamil Nadu, INDIA

Graphical abstract